



THE UNIVERSITY *of* EDINBURGH

Edinburgh Research Explorer

OPEN  ACCESS

Search for CP violation in $D^{(\pm)}$ \rightarrow $(KSK^{(\pm)})K^0$ and $D_s^{(\pm)}$ \rightarrow $K_S^0\pi^{(\pm)}$ decays

RECEIVED: June 11, 2014

REVISED: September 2, 2014

ACCEPTED: September 9, 2014

PUBLISHED: October 3, 2014

Search for CP violation in $D^\pm \rightarrow K_S^0 K^\pm$ and $D_s^\pm \rightarrow K_S^0 \pi^\pm$ decays



The LHCb collaboration

E-mail: gibson@hep.phy.cam.ac.uk

ABSTRACT: A search for CP violation in Cabibbo-suppressed $D^\pm \rightarrow K_S^0 K^\pm$ and $D_s^\pm \rightarrow K_S^0 \pi^\pm$ decays is performed using pp collision data, corresponding to an integrated luminosity of 3 fb^{-1} , recorded by the LHCb experiment. The individual CP -violating asymmetries are measured to be

$$\begin{aligned} \mathcal{A}_{CP}^{D^\pm \rightarrow K_S^0 K^\pm} &= (+0.03 \pm 0.17 \pm 0.14)\% \\ \mathcal{A}_{CP}^{D_s^\pm \rightarrow K_S^0 \pi^\pm} &= (+0.38 \pm 0.46 \pm 0.17)\%, \end{aligned}$$

assuming that CP violation in the Cabibbo-favoured decays is negligible. A combination of the measured asymmetries for the four decay modes $D_{(s)}^\pm \rightarrow K_S^0 K^\pm$ and $D_{(s)}^\pm \rightarrow K_S^0 \pi^\pm$ gives the sum

$$\mathcal{A}_{CP}^{D^\pm \rightarrow K_S^0 K^\pm} + \mathcal{A}_{CP}^{D_s^\pm \rightarrow K_S^0 \pi^\pm} = (+0.41 \pm 0.49 \pm 0.26)\%.$$

In all cases, the first uncertainties are statistical and the second systematic. The results represent the most precise measurements of these asymmetries to date and show no evidence for CP violation.

KEYWORDS: CP violation, Hadron-Hadron Scattering

ARXIV EPRINT: [1406.2624](https://arxiv.org/abs/1406.2624)

Contents

| | | |
|----------|---------------------------------|-----------|
| 1 | Introduction | 1 |
| 2 | Detector and software | 3 |
| 3 | Candidate selection | 3 |
| 4 | Fit method | 5 |
| 5 | Systematic uncertainties | 7 |
| 6 | Results and summary | 10 |
| | The LHCb collaboration | 14 |

1 Introduction

Measurements of CP violation in charm meson decays offer a unique opportunity to search for physics beyond the Standard Model (SM). In the SM, CP violation in the charm sector is expected to be $\mathcal{O}(0.1\%)$ or below [1]. Any enhancement would be an indication of physics beyond the SM. Recent measurements of the difference in CP asymmetries between $D^0 \rightarrow K^+K^-$ and $D^0 \rightarrow \pi^+\pi^-$ decays by the LHCb [2–4], CDF [5], Belle [6] and BaBar [7] collaborations are consistent with SM expectations. Further investigations in other charm decay modes are therefore important to provide a more complete picture of CP violation in the charm sector.

In this paper, CP violation in singly Cabibbo-suppressed $D^\pm \rightarrow K_S^0 K^\pm$ and $D_s^\pm \rightarrow K_S^0 \pi^\pm$ decays is investigated. In the SM, the magnitude of CP violation in these decays is expected to be small, $\mathcal{O}(10^{-4})$, excluding the known contribution from K^0 mixing [8]. If processes beyond the SM contain additional weak phases, other than those contained in the Cabibbo-Kobayashi-Maskawa formalism, additional CP -violating effects could arise [8, 9].

Several searches for CP violation in $D^\pm \rightarrow K_S^0 K^\pm$ and $D_s^\pm \rightarrow K_S^0 \pi^\pm$ decays have been performed previously [10–15]. The CP asymmetry for $D_{(s)}^\pm \rightarrow K_S^0 h^\pm$ decays is defined as

$$\mathcal{A}_{CP}^{D_{(s)}^\pm \rightarrow K_S^0 h^\pm} \equiv \frac{\Gamma(D_{(s)}^+ \rightarrow K_S^0 h^+) - \Gamma(D_{(s)}^- \rightarrow K_S^0 h^-)}{\Gamma(D_{(s)}^+ \rightarrow K_S^0 h^+) + \Gamma(D_{(s)}^- \rightarrow K_S^0 h^-)}, \quad (1.1)$$

where h is a pion or kaon and Γ is the partial decay width. The most precise measurements of the CP asymmetries in the decay modes $D^\pm \rightarrow K_S^0 K^\pm$ and $D_s^\pm \rightarrow K_S^0 \pi^\pm$ are $\mathcal{A}_{CP}^{D^\pm \rightarrow K_S^0 K^\pm} = (-0.25 \pm 0.31)\%$ from the Belle collaboration [14] and $\mathcal{A}_{CP}^{D_s^\pm \rightarrow K_S^0 \pi^\pm} = (+0.61 \pm 0.84)\%$ from the LHCb collaboration [15], respectively. Both measurements are

consistent with CP symmetry. The measurement of $\mathcal{A}_{CP}^{D_s^\pm \rightarrow K_S^0 \pi^\pm}$ by LHCb [15] was performed using data corresponding to an integrated luminosity of 1 fb^{-1} , and is superseded by the result presented here.

In this paper, the CP asymmetries are determined from the measured asymmetries,

$$\mathcal{A}_{\text{meas}}^{D_{(s)}^\pm \rightarrow K_S^0 h^\pm} = \frac{N_{\text{sig}}^{D_{(s)}^+ \rightarrow K_S^0 h^+} - N_{\text{sig}}^{D_{(s)}^- \rightarrow K_S^0 h^-}}{N_{\text{sig}}^{D_{(s)}^+ \rightarrow K_S^0 h^+} + N_{\text{sig}}^{D_{(s)}^- \rightarrow K_S^0 h^-}}, \quad (1.2)$$

where $N_{\text{sig}}^{D_{(s)}^\pm \rightarrow K_S^0 h^\pm}$ is the signal yield in the decay mode $D_{(s)}^\pm \rightarrow K_S^0 h^\pm$. The measured asymmetries include additional contributions other than $\mathcal{A}_{CP}^{D_{(s)}^\pm \rightarrow K_S^0 h^\pm}$, such that, when the considered asymmetries are small, it is possible to approximate

$$\mathcal{A}_{\text{meas}}^{D_{(s)}^\pm \rightarrow K_S^0 h^\pm} \approx \mathcal{A}_{CP}^{D_{(s)}^\pm \rightarrow K_S^0 h^\pm} + \mathcal{A}_{\text{prod}}^{D_{(s)}^\pm} + \mathcal{A}_{\text{det}}^{h^\pm} + \mathcal{A}_{K^0/\bar{K}^0}, \quad (1.3)$$

where $\mathcal{A}_{\text{prod}}^{D_{(s)}^\pm}$ is the asymmetry in the production of $D_{(s)}^\pm$ mesons in high-energy pp collisions in the forward region, and $\mathcal{A}_{\text{det}}^{h^\pm}$ arises from the difference in detection efficiencies between positively and negatively charged hadrons. The asymmetry $\mathcal{A}_{K^0} \equiv (N_{K^0} - N_{\bar{K}^0})/(N_{K^0} + N_{\bar{K}^0}) = -\mathcal{A}_{\bar{K}^0}$, where N_{K^0/\bar{K}^0} is the number of K^0/\bar{K}^0 mesons produced, takes into account the detection asymmetry between a K^0 and a \bar{K}^0 meson due to regeneration and the presence of mixing and CP violation in the K^0 - \bar{K}^0 system. The contribution from the neutral kaon asymmetries is estimated using the method described in ref. [4] and the reconstructed $D_{(s)}^\pm \rightarrow K_S^0 h^\pm$ candidates selected in this analysis. The result $\mathcal{A}_{K^0} = (+0.07 \pm 0.02)\%$ is included as a correction to the measured asymmetries as shown below.

The $D_{(s)}^\pm$ production and hadron detection asymmetries approximately cancel by constructing a *double difference* ($\mathcal{D}\mathcal{D}$) between the four measured asymmetries,

$$\mathcal{A}_{CP}^{\mathcal{D}\mathcal{D}} = \left[\mathcal{A}_{\text{meas}}^{D_s^\pm \rightarrow K_S^0 \pi^\pm} - \mathcal{A}_{\text{meas}}^{D_s^\pm \rightarrow K_S^0 K^\pm} \right] - \left[\mathcal{A}_{\text{meas}}^{D_{(s)}^\pm \rightarrow K_S^0 \pi^\pm} - \mathcal{A}_{\text{meas}}^{D_{(s)}^\pm \rightarrow K_S^0 K^\pm} \right] - 2\mathcal{A}_{K^0}. \quad (1.4)$$

Assuming that CP violation in the Cabibbo-favoured decays is negligible, $\mathcal{A}_{CP}^{\mathcal{D}\mathcal{D}}$ is a measurement of the sum of the CP -violating asymmetries in $D^\pm \rightarrow K_S^0 K^\pm$ and $D_s^\pm \rightarrow K_S^0 \pi^\pm$ decays,

$$\mathcal{A}_{CP}^{D^\pm \rightarrow K_S^0 K^\pm} + \mathcal{A}_{CP}^{D_s^\pm \rightarrow K_S^0 \pi^\pm} = \mathcal{A}_{CP}^{\mathcal{D}\mathcal{D}}. \quad (1.5)$$

The quantity $\mathcal{A}_{CP}^{\mathcal{D}\mathcal{D}}$ provides a measurement that is largely insensitive to production and instrumental asymmetries, even though the CP asymmetries in $D^\pm \rightarrow K_S^0 K^\pm$ and $D_s^\pm \rightarrow K_S^0 \pi^\pm$ decays are expected to have the opposite sign.

The individual CP asymmetries for $D^\pm \rightarrow K_S^0 K^\pm$ and $D_s^\pm \rightarrow K_S^0 \pi^\pm$ decays are also determined using the asymmetry measured in the Cabibbo-favoured decay $D_s^+ \rightarrow \phi \pi^+$,

$$\mathcal{A}_{CP}^{D^\pm \rightarrow K_S^0 K^\pm} = \left[\mathcal{A}_{\text{meas}}^{D^\pm \rightarrow K_S^0 K^\pm} - \mathcal{A}_{\text{meas}}^{D_s^\pm \rightarrow K_S^0 K^\pm} \right] - \left[\mathcal{A}_{\text{meas}}^{D^\pm \rightarrow K_S^0 \pi^\pm} - \mathcal{A}_{\text{meas}}^{D_s^+ \rightarrow \phi \pi^+} \right] - \mathcal{A}_{K^0} \quad (1.6)$$

and

$$\mathcal{A}_{CP}^{D_s^\pm \rightarrow K_S^0 \pi^\pm} = \mathcal{A}_{\text{meas}}^{D_s^\pm \rightarrow K_S^0 \pi^\pm} - \mathcal{A}_{\text{meas}}^{D_s^+ \rightarrow \phi \pi^+} - \mathcal{A}_{K^0}. \quad (1.7)$$

Measurements of the sum $\mathcal{A}_{CP}^{D^\pm \rightarrow K_S^0 K^\pm} + \mathcal{A}_{CP}^{D_s^\pm \rightarrow K_S^0 \pi^\pm}$, and the individual CP asymmetries, $\mathcal{A}_{CP}^{D^\pm \rightarrow K_S^0 K^\pm}$ and $\mathcal{A}_{CP}^{D_s^\pm \rightarrow K_S^0 \pi^\pm}$, are presented in this paper.

2 Detector and software

The LHCb detector [16] is a single-arm forward spectrometer covering the pseudorapidity range $2 < \eta < 5$, designed for the study of particles containing b or c quarks. The detector includes a high-precision tracking system consisting of a silicon-strip vertex detector surrounding the pp interaction region, a large-area silicon-strip detector located upstream of a dipole magnet with a bending power of about 4 Tm, and three stations of silicon-strip detectors and straw drift tubes placed downstream. The polarity of the dipole magnet is reversed periodically throughout data-taking. The combined tracking system provides a momentum measurement with relative uncertainty that varies from 0.4% at 5 GeV/ c to 0.6% at 100 GeV/ c , and impact parameter resolution of 20 μm for tracks with large transverse momentum, p_T . Different types of charged hadrons are distinguished by information from two ring-imaging Cherenkov (RICH) detectors [17]. Photon, electron and hadron candidates are identified by a calorimeter system consisting of scintillating-pad and preshower detectors, an electromagnetic calorimeter and a hadronic calorimeter. Muons are identified by a system composed of alternating layers of iron and multiwire proportional chambers [18]. The trigger [19] consists of a hardware stage, based on information from the calorimeter and muon systems, an inclusive software stage, which uses the tracking system, and a second software stage that exploits the full event reconstruction.

The data used in this analysis corresponds to an integrated luminosity of approximately 3 fb^{-1} recorded in pp collisions at centre-of-mass energies of $\sqrt{s} = 7 \text{ TeV}$ (1 fb^{-1}) and 8 TeV (2 fb^{-1}). Approximately 50% of the data were collected in each configuration (*Up* and *Down*) of the magnet polarity.

In the simulation, pp collisions are generated using PYTHIA 6.4 [20] with a specific LHCb configuration [21]. Decays of hadronic particles are described by EVTGEN [22], in which final state radiation is generated using PHOTOS [23]. The interaction of the generated particles with the detector and its response are implemented using the GEANT4 toolkit [24, 25] as described in ref. [26].

3 Candidate selection

Candidate $D_{(s)}^\pm \rightarrow K_S^0 h^\pm$ and $D_{(s)}^\pm \rightarrow \phi \pi^\pm$ decays are reconstructed from combinations of charged particles that are well-measured, have information in all tracking detectors and are identified as either a pion or kaon, but not as an electron or muon. The primary pp interaction vertex (PV) is chosen to be the one yielding the minimum χ_{IP}^2 of the $D_{(s)}^\pm$ meson, where χ_{IP}^2 is defined as the difference in χ^2 of a given PV reconstructed with and

without the considered particle. The χ_{IP}^2 requirements discussed below are defined with respect to all PVs in the event.

Candidate $D_{(s)}^\pm \rightarrow K_s^0 h^\pm$ decays are reconstructed from a $K_s^0 \rightarrow \pi^+ \pi^-$ decay candidate combined with a charged (bachelor) hadron. The bachelor hadron is required to have $p > 5 \text{ GeV}/c$, $p_T > 0.5 \text{ GeV}/c$ and is classified as a pion or kaon according to the RICH particle identification information. The K_s^0 candidate is formed from a pair of oppositely charged particles, which have $p > 2 \text{ GeV}/c$, $p_T > 0.25 \text{ GeV}/c$, $\chi_{\text{IP}}^2 > 40$, and are identified as pions. The K_s^0 is also required to have a good quality vertex fit, $p_T > 1 \text{ GeV}/c$, $\chi_{\text{IP}}^2 > 7$, a decay vertex separated from the PV by a distance greater than 20 mm, as projected on to the beam direction, and to have a significant flight distance by requiring $\chi_{\text{FD}}^2 > 300$, where χ_{FD}^2 is defined as the increase in the fit χ^2 when the K_s^0 candidate is required to have zero lifetime. The K_s^0 mass is constrained to its known value [27] when the decay vertex is formed and the $D_{(s)}^\pm$ mass calculated. The electron and muon particle identification, flight distance and impact parameter requirements on the K_s^0 reduce backgrounds from semileptonic $D_{(s)}^\pm \rightarrow K_s^0 \ell^\pm \bar{\nu}_\ell$ ($\ell = e$ or μ) and $D_{(s)}^\pm \rightarrow h^\pm h^\mp h^\pm$ decays to a negligible level.

Candidate $D_{(s)}^\pm \rightarrow \phi \pi^\pm$ decays are reconstructed from three charged particles originating from a single vertex. The particles are required to have $\chi_{\text{IP}}^2 > 15$ and a scalar sum $p_T > 2.8 \text{ GeV}/c$. The ϕ candidate is formed from a pair of oppositely charged particles that are identified as kaons and have $p_T > 0.25 \text{ GeV}/c$. The invariant mass of the $K^+ K^-$ pair is required to be within $20 \text{ MeV}/c^2$ of the known ϕ mass [27]. The bachelor pion is required to have $p > 5 \text{ GeV}/c$, $p_T > 0.5 \text{ GeV}/c$ and be identified as a pion.

Candidate $D_{(s)}^\pm$ mesons in all decay modes are required to have $p_T > 1 \text{ GeV}/c$, $\chi_{\text{IP}}^2 < 9$ and vertex χ^2 per degree of freedom less than 10. In addition, the $D_{(s)}^\pm \rightarrow K_s^0 h^\pm$ ($D_{(s)}^\pm \rightarrow \phi \pi^\pm$) candidates are required to have $\chi_{\text{FD}}^2 > 30$ (125), a distance of closest approach of the decay products smaller than 0.6 (0.5) mm, and a cosine of the angle between the $D_{(s)}^\pm$ momentum and the vector between the PV and the $D_{(s)}^\pm$ vertex greater than 0.999. The $D_{(s)}^\pm$ mass is required to be in the range $1.79 < m(K_s^0 h^\pm) < 2.03 \text{ GeV}/c^2$ and $1.805 < m(K^+ K^- \pi^\pm) < 2.035 \text{ GeV}/c^2$ for the $D_{(s)}^\pm \rightarrow K_s^0 h^\pm$ and $D_{(s)}^\pm \rightarrow \phi \pi^\pm$ decays, respectively.

Figures 1 and 2 show the mass distributions of selected $D_{(s)}^\pm \rightarrow K_s^0 h^\pm$ and $D_{(s)}^\pm \rightarrow \phi \pi^\pm$ candidates for data taken in the magnet polarity *Up* configuration at $\sqrt{s} = 8 \text{ TeV}$. The mass distributions for the magnet polarity *Down* configuration are approximately equal.

Three categories of background contribute to the selected $D_{(s)}^\pm$ candidates. A *low-mass* background contributes at low $D_{(s)}^\pm$ mass and corresponds to decay modes such as $D^\pm \rightarrow K_s^0 \pi^\pm \pi^0$ and $D_s^\pm \rightarrow K^\mp K^\pm \pi^\pm \pi^0$, where the π^0 is not reconstructed, for $D_{(s)}^\pm \rightarrow K_s^0 h^\pm$ and $D_{(s)}^\pm \rightarrow \phi \pi^\pm$ decays, respectively. A *cross-feed* background contributes to $D_{(s)}^\pm \rightarrow K_s^0 h^\pm$ decays and arises from $D_{(s)}^\pm \rightarrow K_s^0 h^\pm$ decays in which the bachelor pion (kaon) is misidentified as a kaon (pion). Simulation studies show that the misidentification of the bachelor pion in $D^\pm \rightarrow K_s^0 \pi^\pm$ decays produces a cross-feed background that extends under the $D_s^\pm \rightarrow K_s^0 K^\pm$ signal peak, and that the bachelor kaon in $D_s^\pm \rightarrow K_s^0 K^\pm$ decays produces a small complementary cross-feed background that extends under the $D^\pm \rightarrow K_s^0 \pi^\pm$ signal peak. A *combinatorial* background contribution is present in both $D_{(s)}^\pm \rightarrow K_s^0 h^\pm$ and

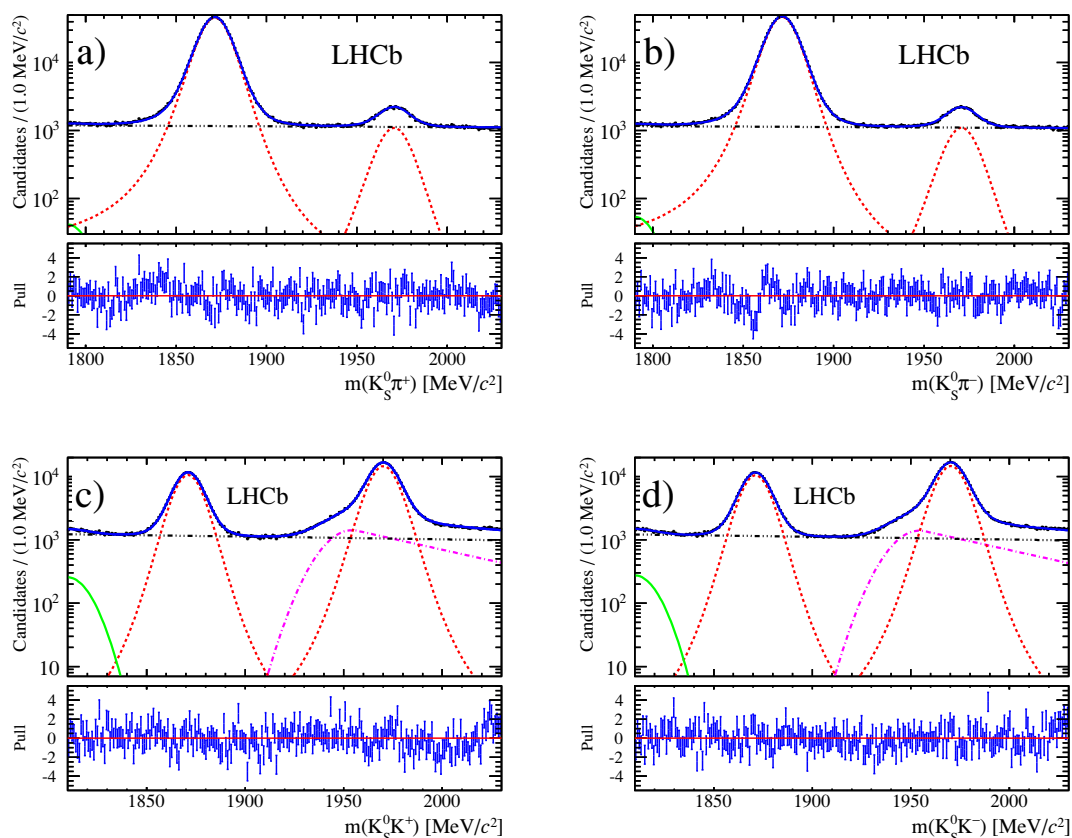


Figure 1. Invariant mass distributions for the a) $D_{(s)}^+ \rightarrow K_S^0 \pi^+$, b) $D_{(s)}^- \rightarrow K_S^0 \pi^-$, c) $D_{(s)}^+ \rightarrow K_S^0 K^+$ and d) $D_{(s)}^- \rightarrow K_S^0 K^-$ decay candidates for data taken in the magnetic polarity Up configuration at $\sqrt{s} = 8$ TeV. The data are shown as black points and the total fit function by a blue line. The contributions from the signal and the low-mass, cross-feed and combinatorial backgrounds are indicated by red (dotted), green (full), magenta (dash-dotted) and black (multiple-dot-dashed) lines, respectively. The bottom figures are the normalised residuals (pull) distributions.

$D_{(s)}^\pm \rightarrow \phi \pi^\pm$ decay modes. Background from Λ_c^\pm decays with a proton in the final state, and $D_{(s)}^\pm$ mesons originating from the decays of b hadrons are neglected in the fit and considered when assessing systematic uncertainties.

4 Fit method

The yields and asymmetries for the $D_{(s)}^\pm \rightarrow K_S^0 \pi^\pm$, $D_{(s)}^\pm \rightarrow K_S^0 K^\pm$, and $D_{(s)}^\pm \rightarrow \phi \pi^\pm$ signal channels and the various backgrounds are determined from a likelihood fit to the respective binned invariant mass distribution. For each final state, the data are divided into four independent subsamples, according to magnet polarity and candidate charge, and a simultaneous fit is performed. The $\sqrt{s} = 7$ TeV and 8 TeV data sets are fitted separately to take into account background rate and data-taking conditions.

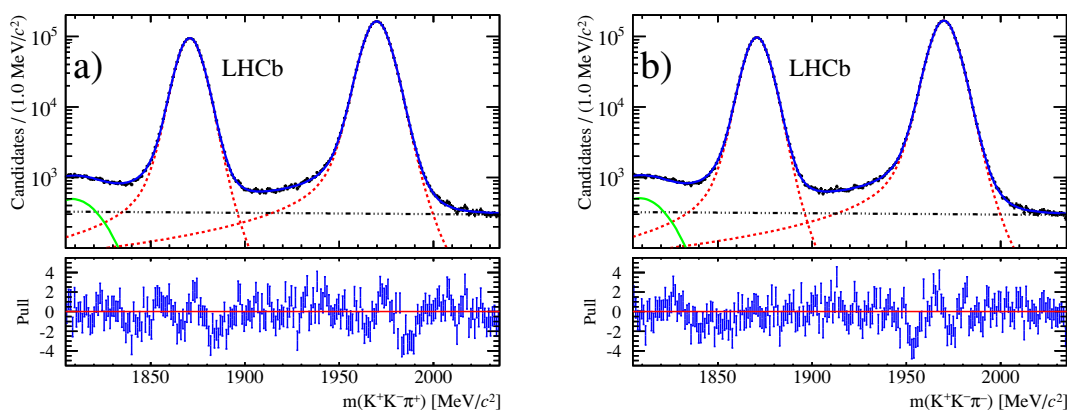


Figure 2. Invariant mass distributions for the a) $D_{(s)}^+ \rightarrow \phi\pi^+$ and b) $D_{(s)}^- \rightarrow \phi\pi^-$ decay candidates for data taken in the magnet polarity Up configuration at $\sqrt{s} = 8$ TeV. The data are shown as black points and the total fit function by a blue line. The contributions from the signal and the low-mass and combinatorial backgrounds are indicated by red (dotted), green (full) and black (multiple-dashed) lines, respectively. The bottom figures are the normalised residuals (pull) distributions.

All signal and background mass shapes are determined using simulated data samples. The $D_{(s)}^\pm \rightarrow K_s^0 h^\pm$ signal shape is described by the parametric function,

$$f(m) \propto \exp \left[\frac{-(m - \mu)^2}{2\sigma^2 + (m - \mu)^2 \alpha_{L,R}} \right], \quad (4.1)$$

which is parametrised by a mean μ , width σ and asymmetric low- and high-mass tail parameters, α_L (for $m < \mu$) and α_R (for $m > \mu$), respectively. The means and widths of the four $D_{(s)}^\pm$ signal peaks are allowed to vary in the fit. In addition, 3 tail parameters are included in the fit. All the $D_{(s)}^\pm \rightarrow K_s^0 \pi^\pm$ signal peaks are described by two common α_L and α_R tail parameters, whereas for the $D_{(s)}^\pm \rightarrow K_s^0 K^\pm$ signal peaks α_L and α_R are set to be equal and a single tail parameter is used. The widths and tail parameters are also common for the two magnet polarities.

The low-mass background is modelled by a Gaussian function with a fixed mean ($1790 \text{ MeV}/c^2$ and $1810 \text{ MeV}/c^2$ for $D_{(s)}^\pm \rightarrow K_s^0 \pi^\pm$ and $D_{(s)}^\pm \rightarrow K_s^0 K^\pm$, respectively) and width ($10 \text{ MeV}/c^2$), as determined from simulation. The cross-feed components are described by a Crystal Ball function [28] with tail parameters fixed to those obtained in the simulation. Since the cross-feed contribution from $D_s^\pm \rightarrow K_s^0 K^\pm$ is very small compared to the $D^\pm \rightarrow K_s^0 \pi^\pm$ signal, the width and mean of this contribution are also taken from simulation. The cross-feed contribution from $D^\pm \rightarrow K_s^0 \pi^\pm$ to $D_s^\pm \rightarrow K_s^0 K^\pm$ candidates extends under the signal peak to low- and high-mass. The mean and width of the Crystal Ball function are allowed to vary in the fit with a common width for the two magnet polarities. The combinatorial background is described by a linear term with a slope free to vary for all mass distributions.

| Decay mode | Yield |
|-------------------------------------|------------------------|
| $D^\pm \rightarrow K_S^0 \pi^\pm$ | 4 834 440 \pm 2 555 |
| $D_s^\pm \rightarrow K_S^0 \pi^\pm$ | 120 976 \pm 692 |
| $D^\pm \rightarrow K_S^0 K^\pm$ | 1 013 516 \pm 1 379 |
| $D_s^\pm \rightarrow K_S^0 K^\pm$ | 1 476 980 \pm 2 354 |
| $D^+ \rightarrow \phi \pi^+$ | 7 020 160 \pm 2 739 |
| $D_s^+ \rightarrow \phi \pi^+$ | 13 144 900 \pm 3 879 |

Table 1. Signal yields.

The $D_{(s)}^\pm \rightarrow \phi \pi^\pm$ signal peaks are described by the sum of eq. (4.1) and a Crystal Ball function. The means and widths of the four $D_{(s)}^\pm$ signal peaks and a common Crystal Ball width are allowed to vary in the fit. In addition, five tail parameters are included in the fit. These are α_L for the D^\pm and D_s^\pm signal peaks and a single offset $\Delta\alpha \equiv \alpha_L - \alpha_R$, and two Crystal Ball tail parameters. The widths and tail parameters are common for the two magnet polarities. The low-mass background is modelled with a Gaussian function and the combinatorial background is described by a linear term with a slope free to vary for all mass distributions.

To reduce any bias in the measured asymmetries due to potential detection and production asymmetries arising from the difference in the kinematic properties of the $D_{(s)}^\pm$ or the bachelor hadron, the p_T and η distributions of the $D_{(s)}^\pm$ candidate for the $D_{(s)}^\pm \rightarrow K_S^0 \pi^\pm$ and $D_{(s)}^\pm \rightarrow \phi \pi^\pm$ decay modes are weighted to be consistent with those of the $D_{(s)}^\pm \rightarrow K_S^0 K^\pm$ candidates. To further reduce a potential bias due to a track detection asymmetry, an unweighted average of the asymmetries measured using the two magnet polarity configurations is determined.

The total fitted signal yields for all decay modes and the measured and calculated CP asymmetries are summarised in table 1 and table 2, respectively. Since the correlation between the measured asymmetries is negligible, the CP asymmetries are calculated assuming they are uncorrelated.

5 Systematic uncertainties

The values of the CP asymmetries \mathcal{A}_{CP}^{DD} , $\mathcal{A}_{CP}^{D^\pm \rightarrow K_S^0 K^\pm}$ and $\mathcal{A}_{CP}^{D_s^\pm \rightarrow K_S^0 \pi^\pm}$ are subject to several sources of systematic uncertainty arising from the fitting procedure, treatment of the backgrounds, and trigger- and detector-related effects. A summary of the contributions to the systematic uncertainties is given in table 3.

The systematic uncertainty due to the fit procedure is evaluated by replacing the description of the $D_{(s)}^\pm \rightarrow K_S^0 h^\pm$ and $D_{(s)}^\pm \rightarrow \phi \pi^\pm$ signal, combinatorial background and low-mass background in the fit with alternative parameterizations. The systematic uncertainty is calculated by comparing the asymmetries after each change in the fit function to

| Asymmetry | $\sqrt{s} = 7 \text{ TeV}$ | | $\sqrt{s} = 8 \text{ TeV}$ | | Total |
|---|----------------------------|------------------|----------------------------|------------------|------------------|
| | Up | $Down$ | Up | $Down$ | |
| $\mathcal{A}_{\text{meas}}^{D^\pm \rightarrow K_S^0 \pi^\pm}$ | -1.04 ± 0.19 | -0.74 ± 0.16 | -0.88 ± 0.08 | -1.04 ± 0.08 | -0.95 ± 0.05 |
| $\mathcal{A}_{\text{meas}}^{D_s^\pm \rightarrow K_S^0 \pi^\pm}$ | $+2.55 \pm 1.34$ | -0.56 ± 1.09 | -0.46 ± 0.78 | -0.66 ± 0.77 | -0.15 ± 0.46 |
| $\mathcal{A}_{\text{meas}}^{D^\pm \rightarrow K_S^0 K^\pm}$ | -0.47 ± 0.59 | -0.23 ± 0.50 | -0.11 ± 0.32 | $+0.38 \pm 0.31$ | $+0.01 \pm 0.19$ |
| $\mathcal{A}_{\text{meas}}^{D_s^\pm \rightarrow K_S^0 K^\pm}$ | $+0.28 \pm 0.34$ | $+0.84 \pm 0.28$ | -0.69 ± 0.18 | $+1.02 \pm 0.17$ | $+0.27 \pm 0.11$ |
| $\mathcal{A}_{\text{meas}}^{D_s^+ \rightarrow \phi \pi^+}$ | -1.02 ± 0.09 | $+0.24 \pm 0.07$ | -0.71 ± 0.05 | -0.48 ± 0.05 | -0.41 ± 0.05 |
| \mathcal{A}_{CP}^{DD} | $+2.71 \pm 1.46$ | -1.04 ± 1.18 | $+0.86 \pm 0.82$ | -0.39 ± 0.81 | $+0.41 \pm 0.49$ |
| $\mathcal{A}_{CP}^{D^\pm \rightarrow K_S^0 K^\pm}$ | -0.80 ± 0.53 | -0.17 ± 0.44 | $+0.69 \pm 0.27$ | -0.14 ± 0.27 | $+0.03 \pm 0.17$ |
| $\mathcal{A}_{CP}^{D_s^\pm \rightarrow K_S^0 \pi^\pm}$ | $+3.51 \pm 1.35$ | -0.87 ± 1.09 | $+0.17 \pm 0.78$ | -0.25 ± 0.77 | $+0.38 \pm 0.46$ |

Table 2. Measured asymmetries (in %) for the decay modes $D^\pm \rightarrow K_S^0 \pi^\pm$, $D_s^\pm \rightarrow K_S^0 \pi^\pm$, $D_s^\pm \rightarrow K_S^0 K^\pm$ and $D_s^+ \rightarrow \phi \pi^+$ and the calculated CP asymmetries. The results are reported separately for $\sqrt{s} = 7 \text{ TeV}$ and $\sqrt{s} = 8 \text{ TeV}$ data and the two magnetic polarities (Up and $Down$). The combined results are given in the final column. The quoted uncertainties are statistical only.

| Source | $\sqrt{s} = 7 \text{ TeV}$ | | | $\sqrt{s} = 8 \text{ TeV}$ | | |
|---------------------|----------------------------|--|--|----------------------------|--|--|
| | \mathcal{A}_{CP}^{DD} | $\mathcal{A}_{CP}^{D^\pm \rightarrow K_S^0 K^\pm}$ | $\mathcal{A}_{CP}^{D_s^\pm \rightarrow K_S^0 \pi^\pm}$ | \mathcal{A}_{CP}^{DD} | $\mathcal{A}_{CP}^{D^\pm \rightarrow K_S^0 K^\pm}$ | $\mathcal{A}_{CP}^{D_s^\pm \rightarrow K_S^0 \pi^\pm}$ |
| Fit procedure | 0.14 | 0.09 | 0.11 | 0.07 | 0.05 | 0.01 |
| Cross-feed bkgd. | 0.03 | 0.01 | 0.02 | 0.01 | – | 0.01 |
| Non-prompt charm | 0.01 | – | – | 0.01 | – | – |
| Kinematic weighting | 0.08 | 0.06 | 0.13 | 0.05 | 0.07 | 0.12 |
| Kinematic region | 0.10 | 0.06 | 0.04 | 0.19 | 0.02 | 0.17 |
| Trigger | 0.13 | 0.13 | 0.07 | 0.17 | 0.17 | 0.09 |
| K^0 asymmetry | 0.03 | 0.02 | 0.02 | 0.04 | 0.02 | 0.02 |
| Total | 0.23 | 0.18 | 0.19 | 0.27 | 0.19 | 0.22 |

Table 3. Systematic uncertainties (absolute values in %) on the CP asymmetries for $\sqrt{s} = 7$ and 8 TeV data. The total systematic uncertainty is the sum in quadrature of the individual contributions.

those obtained without the modification. The overall systematic uncertainty due to the fit procedure is calculated assuming that the individual contributions are entirely correlated.

The systematic uncertainty due to the $D_s^\pm \rightarrow K_S^0 K^\pm$ cross-feed in the $D_{(s)}^\pm \rightarrow K_S^0 \pi^\pm$ fit is determined by repeating the fit with the cross-feed component yields fixed to those from an estimation based on particle identification efficiencies determined from a large sample of $D^{*\pm} \rightarrow D \pi^\pm$ decays, where D is a D^0 or \bar{D}^0 meson [29]. In the $D_{(s)}^\pm \rightarrow K_S^0 K^\pm$ fit, the $D^\pm \rightarrow K_S^0 \pi^\pm$ cross-feed shape tail parameters are allowed to vary. The systematic uncertainty is taken as the shift in the central values of the CP asymmetries.

The systematic uncertainty due to the presence of charm backgrounds, such as $\Lambda_c^\pm \rightarrow \Lambda^0 h^\pm$ and $\Lambda_c^\pm \rightarrow K_s^0 p$, which have a proton in the final state, is investigated by applying a proton identification veto on all final state tracks in the $D_{(s)}^\pm \rightarrow K_s^0 h^\pm$ data sample. The effect is to reduce the total number of $D_{(s)}^\pm \rightarrow K_s^0 h^\pm$ candidates, without a significant shift in the asymmetries. This source of systematic uncertainty is therefore considered negligible.

In the selection of $D_{(s)}^\pm$ candidates, the χ_{IP}^2 requirement on the $D_{(s)}^\pm$ removes the majority of background from secondary $D_{(s)}^\pm$ mesons originating from the decay of a b hadron. The remaining secondary $D_{(s)}^\pm$ mesons may introduce a bias in the measured CP asymmetries due to a difference in the production asymmetries for b hadrons and $D_{(s)}^\pm$ mesons. In order to investigate this bias, the $D_{(s)}^\pm$ production asymmetries in eq. (1.3) for $D_{(s)}^\pm \rightarrow K_s^0 h^\pm$ decays, and similarly for $D_{(s)}^\pm \rightarrow \phi \pi^\pm$ decays, are modified using

$$\mathcal{A}_{\text{prod}}^{D_{(s)}^\pm}(\text{corr}) = \frac{\mathcal{A}_{\text{prod}}^{D_{(s)}^\pm} + f \mathcal{A}_{\text{prod}}^B}{1 + f}, \quad (5.1)$$

where f is the fraction of secondary $D_{(s)}^\pm$ candidates in a particular decay channel and $\mathcal{A}_{\text{prod}}^B$ is the corresponding b -hadron production asymmetry. The fraction f is estimated from the measured D^\pm , D_s^\pm and b hadron inclusive cross-sections [30, 31], the inclusive branching fractions $\mathcal{B}(b \rightarrow D^\pm X)$ and $\mathcal{B}(b \rightarrow D_s^\pm X)$, where X corresponds to any other particles in the final state [27], the exclusive branching fractions $\mathcal{B}(D_{(s)}^\pm \rightarrow K_s^0 h^\pm)$ and $\mathcal{B}(D_{(s)}^\pm \rightarrow \phi \pi^\pm)$ [27], and the efficiencies estimated from simulation. The resulting values of f lie in the range 1.3 – 3.2%. The b -hadron production asymmetry $\mathcal{A}_{\text{prod}}^B$ is taken to be $(-1.5 \pm 1.3)\%$, consistent with measurements of the B^+ and B^0 production asymmetries in pp collisions in the forward region [32]. The effect of the uncertainty on $\mathcal{A}_{\text{prod}}^B$ is negligible. The systematic uncertainty is evaluated by using the modified $D_{(s)}^\pm$ production asymmetries from eq. (5.1) for each of the decay modes and recalculating the CP asymmetries.

The effect on the CP asymmetries of weighting the $D_{(s)}^\pm \rightarrow K_s^0 \pi^\pm$ and $D_{(s)}^\pm \rightarrow \phi \pi^\pm$ candidates using the $D_{(s)}^\pm$ kinematic distributions compared to the unweighted results is assigned as a systematic uncertainty. The effect of the weighting procedure on the bachelor hadron kinematic distributions is also investigated by comparing the bachelor p_T and η distributions before and after weighting. The results show excellent agreement and no further systematic uncertainty is assigned.

Due to a small intrinsic left-right detection asymmetry, for a given magnet polarity, an excess of either positively or negatively charged bachelor hadrons is detected at large η and small p , where p is the component of momentum parallel to the LHCb beam-axis [33]. This excess leads to charge asymmetries, which may not completely cancel in the analysis when the average of the *Up* and *Down* magnet polarity asymmetries is calculated. To investigate this effect, $D_{(s)}^\pm$ candidates, whose bachelor hadron falls within the above kinematic region, are removed and the resulting asymmetries compared to those without the selection criterion applied. The kinematic region excluded is the same as that used in refs. [33, 34] and removes $\sim 3\%$ of the $D_{(s)}^\pm$ candidates. The difference between the asymmetries is taken to be the systematic uncertainty.

Detector related systematic uncertainties may also arise from the variation of operating conditions between data-taking periods, and data not taken concurrently with the two magnet polarities. A consistency check is therefore performed by dividing the data into 12 subsamples with similar size, corresponding to data-taking periods and magnet polarity changes, and the analysis is repeated for each subsample. The asymmetries obtained are consistent and no further systematic uncertainty is assigned.

Potential trigger biases are studied using a large sample of $D^\pm \rightarrow K^\mp \pi^\pm \pi^\pm$ decays with the $D_{(s)}^\pm \rightarrow \phi \pi^\pm$ selection criteria applied. The data are divided into subsamples, corresponding to various hardware trigger configurations, and the asymmetries for the individual subsamples measured. A systematic uncertainty is assigned, which corresponds to the maximum deviation of a CP asymmetry from a single subsample compared to the mean asymmetry from all subsamples, assuming there is no cancellation when the CP asymmetries are remeasured.

In $D_{(s)}^\pm \rightarrow K_S^0 h^\pm$ decays, the K_S^0 meson originates from the production of a neutral kaon flavour eigenstate (K^0 or \bar{K}^0) in the decay of the $D_{(s)}^\pm$ meson. The neutral kaon state evolves, via mixing and CP violation, and interacts with the detector material creating an asymmetry in the reconstruction before decaying. The overall effect is estimated using simulation, as described in ref. [4], and a correction is applied to the calculated asymmetries as shown in eqs. (1.5)–(1.7). The full uncertainty of the estimated effect is assigned as a systematic uncertainty.

6 Results and summary

A search for CP violation in $D^\pm \rightarrow K_S^0 K^\pm$ and $D_s^\pm \rightarrow K_S^0 \pi^\pm$ decays is performed using a data sample of pp collisions, corresponding to an integrated luminosity of 3 fb^{-1} at centre-of-mass energies of 7 TeV (1 fb^{-1}) and 8 TeV (2 fb^{-1}), recorded by the LHCb experiment. The results for the two centre-of-mass energies are combined using the method described in ref. [35], assuming all the systematic uncertainties are correlated. The individual CP -violating asymmetries are measured to be

$$\mathcal{A}_{CP}^{D^\pm \rightarrow K_S^0 K^\pm} = (+0.03 \pm 0.17 \pm 0.14)\%$$

and

$$\mathcal{A}_{CP}^{D_s^\pm \rightarrow K_S^0 \pi^\pm} = (+0.38 \pm 0.46 \pm 0.17)\%,$$

assuming that CP violation in the Cabibbo-favoured decay is negligible. The measurements are consistent with previous results [14, 15], and $\mathcal{A}_{CP}^{D_s^\pm \rightarrow K_S^0 \pi^\pm}$ supersedes the result reported in ref. [15], which used a subsample of the present data.

A combination of the measured asymmetries for the four decay modes $D_{(s)}^\pm \rightarrow K_S^0 K^\pm$ and $D_{(s)}^\pm \rightarrow K_S^0 \pi^\pm$ gives the sum

$$\mathcal{A}_{CP}^{D^\pm \rightarrow K_S^0 K^\pm} + \mathcal{A}_{CP}^{D_s^\pm \rightarrow K_S^0 \pi^\pm} = (+0.41 \pm 0.49 \pm 0.26)\%,$$

and provides a measurement that is largely insensitive to production and instrumental asymmetries. In all cases, the first uncertainties are statistical and the second are systematic. The results represent the most precise measurements of these quantities to date and show no evidence for CP violation.

Acknowledgments

We express our gratitude to our colleagues in the CERN accelerator departments for the excellent performance of the LHC. We thank the technical and administrative staff at the LHCb institutes. We acknowledge support from CERN and from the national agencies: CAPES, CNPq, FAPERJ and FINEP (Brazil); NSFC (China); CNRS/IN2P3 (France); BMBF, DFG, HGF and MPG (Germany); SFI (Ireland); INFN (Italy); FOM and NWO (The Netherlands); MNiSW and NCN (Poland); MEN/IFA (Romania); MinES and FANO (Russia); MinECo (Spain); SNSF and SER (Switzerland); NASU (Ukraine); STFC (United Kingdom); NSF (U.S.A.). The Tier1 computing centres are supported by IN2P3 (France), KIT and BMBF (Germany), INFN (Italy), NWO and SURF (The Netherlands), PIC (Spain), GridPP (United Kingdom). We are indebted to the communities behind the multiple open source software packages on which we depend. We are also thankful for the computing resources and the access to software R&D tools provided by Yandex LLC (Russia). Individual groups or members have received support from EPLANET, Marie Skłodowska-Curie Actions and ERC (European Union), Conseil général de Haute-Savoie, Labex ENIGMASS and OCEVU, Région Auvergne (France), RFBR (Russia), XuntaGal and GENCAT (Spain), Royal Society and Royal Commission for the Exhibition of 1851 (United Kingdom).

Open Access. This article is distributed under the terms of the Creative Commons Attribution License ([CC-BY 4.0](https://creativecommons.org/licenses/by/4.0/)), which permits any use, distribution and reproduction in any medium, provided the original author(s) and source are credited.

References

- [1] S. Bianco, F.L. Fabbri, D. Benson and I. Bigi, *A Cicerone for the physics of charm*, *Riv. Nuovo Cim.* **26N7** (2003) 1 [[hep-ex/0309021](#)] [[INSPIRE](#)].
- [2] LHCb collaboration, *A search for time-integrated CP-violation in $D^0 \rightarrow K^- K^+$ and $D^0 \rightarrow \pi^- \pi^+$ decays*, *LHCb-CONF-2013-003*, CERN, Geneva Switzerland (2013).
- [3] LHCb collaboration, *Search for direct CP violation in $D^0 \rightarrow h^- h^+$ modes using semileptonic B decays*, *Phys. Lett.* **B 723** (2013) 33 [[arXiv:1303.2614](#)] [[INSPIRE](#)].
- [4] LHCb collaboration, *Measurement of CP asymmetry in $D^0 \rightarrow K^- K^+$ and $D^0 \rightarrow \pi^- \pi^+$ decays*, *JHEP* **07** (2014) 041 [[arXiv:1405.2797](#)] [[INSPIRE](#)].
- [5] CDF collaboration, T. Aaltonen et al., *Measurement of the difference of CP-violating asymmetries in $D^0 \rightarrow K^+ K^-$ and $D^0 \rightarrow \pi^+ \pi^-$ decays at CDF*, *Phys. Rev. Lett.* **109** (2012) 111801 [[arXiv:1207.2158](#)] [[INSPIRE](#)].
- [6] BELLE collaboration, B.R. Ko, *Direct CP-violation in charm at Belle*, *PoS(ICHEP2012)353* [[arXiv:1212.1975](#)] [[INSPIRE](#)].

- [7] BABAR collaboration, B. Aubert et al., *Search for CP-violation in the decays $D^0 \rightarrow K^- K^+$ and $D^0 \rightarrow \pi^- \pi^+$* , *Phys. Rev. Lett.* **100** (2008) 061803 [[arXiv:0709.2715](#)] [[INSPIRE](#)].
- [8] H.J. Lipkin and Z.-Z. Xing, *Flavor symmetry, K^0 - \bar{K}^0 mixing and new physics effects on CP-violation in D^\pm and D_s^\pm decays*, *Phys. Lett. B* **450** (1999) 405 [[hep-ph/9901329](#)] [[INSPIRE](#)].
- [9] B. Bhattacharya, M. Gronau and J.L. Rosner, *CP asymmetries in singly-Cabibbo-suppressed D decays to two pseudoscalar mesons*, *Phys. Rev. D* **85** (2012) 054014 [[arXiv:1201.2351](#)] [[INSPIRE](#)].
- [10] FOCUS collaboration, J.M. Link et al., *Search for CP-violation in the decays $D^+ \rightarrow K_S \pi^+$ and $D^+ \rightarrow K_S K^+$* , *Phys. Rev. Lett.* **88** (2002) 041602 [Erratum *ibid.* **88** (2002) 159903] [[hep-ex/0109022](#)] [[INSPIRE](#)].
- [11] CLEO collaboration, H. Mendez et al., *Measurements of D meson decays to two pseudoscalar mesons*, *Phys. Rev. D* **81** (2010) 052013 [[arXiv:0906.3198](#)] [[INSPIRE](#)].
- [12] BELLE collaboration, B.R. Ko et al., *Search for CP-violation in the decays $D_{(s)}^+ \rightarrow K_S^0 \pi^+$ and $D_{(s)}^+ \rightarrow K_S^0 K^+$* , *Phys. Rev. Lett.* **104** (2010) 181602 [[arXiv:1001.3202](#)] [[INSPIRE](#)].
- [13] BABAR collaboration, J.P. Lees et al., *Search for CP-violation in the decays $D^\pm \rightarrow K_S^0 K^\pm$, $D_s^\pm \rightarrow K_S^0 K^\pm$ and $D_s^\pm \rightarrow K_S^0 \pi^\pm$* , *Phys. Rev. D* **87** (2013) 052012 [[arXiv:1212.3003](#)] [[INSPIRE](#)].
- [14] BELLE collaboration, B.R. Ko et al., *Search for CP-violation in the decay $D^+ \rightarrow K_S^0 K^+$* , *JHEP* **02** (2013) 098 [[arXiv:1212.6112](#)] [[INSPIRE](#)].
- [15] LHCb collaboration, *Search for CP violation in $D^+ \rightarrow \phi \pi^+$ and $D_s^+ \rightarrow K_S^0 \pi^+$ decays*, *JHEP* **06** (2013) 112 [[arXiv:1303.4906](#)] [[INSPIRE](#)].
- [16] LHCb collaboration, *The LHCb detector at the LHC, 2008 JINST* **3** S08005 [[INSPIRE](#)].
- [17] LHCb RICH GROUP collaboration, M. Adinolfi et al., *Performance of the LHCb RICH detector at the LHC*, *Eur. Phys. J. C* **73** (2013) 2431 [[arXiv:1211.6759](#)] [[INSPIRE](#)].
- [18] A.A. Alves Jr. et al., *Performance of the LHCb muon system, 2013 JINST* **8** P02022 [[arXiv:1211.1346](#)] [[INSPIRE](#)].
- [19] R. Aaij et al., *The LHCb trigger and its performance in 2011, 2013 JINST* **8** P04022 [[arXiv:1211.3055](#)] [[INSPIRE](#)].
- [20] T. Sjöstrand, S. Mrenna and P.Z. Skands, *PYTHIA 6.4 physics and manual*, *JHEP* **05** (2006) 026 [[hep-ph/0603175](#)] [[INSPIRE](#)].
- [21] I. Belyaev et al., *Handling of the generation of primary events in GAUSS, the LHCb simulation framework*, *IEEE Nucl. Sci. Symp. Conf. Rec.* (2010) 1155 [[INSPIRE](#)].
- [22] D.J. Lange, *The EvtGen particle decay simulation package*, *Nucl. Instrum. Meth. A* **462** (2001) 152 [[INSPIRE](#)].
- [23] P. Golonka and Z. Was, *PHOTOS Monte Carlo: a precision tool for QED corrections in Z and W decays*, *Eur. Phys. J. C* **45** (2006) 97 [[hep-ph/0506026](#)] [[INSPIRE](#)].
- [24] J. Allison et al., *GEANT4 developments and applications*, *IEEE Trans. Nucl. Sci.* **53** (2006) 270 [[INSPIRE](#)].
- [25] GEANT4 collaboration, S. Agostinelli et al., *GEANT4: a simulation toolkit*, *Nucl. Instrum. Meth. A* **506** (2003) 250 [[INSPIRE](#)].

- [26] LHCb collaboration, *The LHCb simulation application, Gauss: design, evolution and experience*, *J. Phys. Conf. Ser.* **331** (2011) 032023 [INSPIRE].
- [27] PARTICLE DATA GROUP collaboration, J. Beringer et al., *Review of particle physics (RPP)*, *Phys. Rev. D* **86** (2012) 010001 [INSPIRE] and 2013 partial update for the 2014 edition.
- [28] T. Skwarnicki, *A study of the radiative cascade transitions between the Υ' and Υ resonances*, Ph.D. thesis, Institute of Nuclear Physics, Krakow Poland (1986) [INSPIRE].
- [29] A. Powell et al., *Particle identification at LHCb*, LHCb-PROC-2011-008, CERN, Geneva Switzerland (2011) [PoS(ICHEP 2010)020].
- [30] LHCb collaboration, *Prompt charm production in pp collisions at $\sqrt{s} = 7$ TeV*, *Nucl. Phys. B* **871** (2013) 1 [arXiv:1302.2864] [INSPIRE].
- [31] LHCb collaboration, *Measurement of $\sigma(pp \rightarrow b\bar{b}X)$ at $\sqrt{s} = 7$ TeV in the forward region*, *Phys. Lett. B* **694** (2010) 209 [arXiv:1009.2731] [INSPIRE].
- [32] LHCb collaboration, *Observation of CP-violation in $B^\pm \rightarrow DK^\pm$ decays*, *Phys. Lett. B* **712** (2012) 203 [Erratum *ibid.* **713** (2012) 351] [arXiv:1203.3662] [INSPIRE].
- [33] LHCb collaboration, *Measurement of the $D_s^+ - D_s^-$ production asymmetry in 7 TeV pp collisions*, *Phys. Lett. B* **713** (2012) 186 [arXiv:1205.0897] [INSPIRE].
- [34] LHCb collaboration, *Measurement of the D^\pm production asymmetry in 7 TeV pp collisions*, *Phys. Lett. B* **718** (2013) 902 [arXiv:1210.4112] [INSPIRE].
- [35] L. Lyons, D. Gibaut and P. Clifford, *How to combine correlated estimates of a single physical quantity*, *Nucl. Instrum. Meth. A* **270** (1988) 110 [INSPIRE].

The LHCb collaboration

R. Aaij⁴¹, B. Adeva³⁷, M. Adinolfi⁴⁶, A. Affolder⁵², Z. Ajaltouni⁵, S. Akar⁶, J. Albrecht⁹, F. Alessio³⁸, M. Alexander⁵¹, S. Ali⁴¹, G. Alkhazov³⁰, P. Alvarez Cartelle³⁷, A.A. Alves Jr^{25,38}, S. Amato², S. Amerio²², Y. Amhis⁷, L. An³, L. Anderlini^{17,g}, J. Anderson⁴⁰, R. Andreassen⁵⁷, M. Andreotti^{16,f}, J.E. Andrews⁵⁸, R.B. Appleby⁵⁴, O. Aquines Gutierrez¹⁰, F. Archilli³⁸, A. Artamonov³⁵, M. Artuso⁵⁹, E. Aslanides⁶, G. Auriemma^{25,n}, M. Baalouch⁵, S. Bachmann¹¹, J.J. Back⁴⁸, A. Badalov³⁶, V. Balagura³¹, W. Baldini¹⁶, R.J. Barlow⁵⁴, C. Barschel³⁸, S. Barsuk⁷, W. Barter⁴⁷, V. Batozskaya²⁸, V. Battista³⁹, A. Bay³⁹, L. Beaucourt⁴, J. Beddow⁵¹, F. Bedeschi²³, I. Bediaga¹, S. Belogurov³¹, K. Belous³⁵, I. Belyaev³¹, E. Ben-Haim⁸, G. Bencivenni¹⁸, S. Benson³⁸, J. Benton⁴⁶, A. Berezhnoy³², R. Bernet⁴⁰, M.-O. Bettler⁴⁷, M. van Beuzekom⁴¹, A. Bien¹¹, S. Bifani⁴⁵, T. Bird⁵⁴, A. Bizzeti^{17,i}, P.M. Bjørnstad⁵⁴, T. Blake⁴⁸, F. Blanc³⁹, J. Blouw¹⁰, S. Blusk⁵⁹, V. Bocci²⁵, A. Bondar³⁴, N. Bondar^{30,38}, W. Bonivento^{15,38}, S. Borghi⁵⁴, A. Borgia⁵⁹, M. Borsato⁷, T.J.V. Bowcock⁵², E. Bowen⁴⁰, C. Bozzi¹⁶, T. Brambach⁹, J. van den Brand⁴², J. Bressieux³⁹, D. Brett⁵⁴, M. Britsch¹⁰, T. Britton⁵⁹, J. Brodzicka⁵⁴, N.H. Brook⁴⁶, H. Brown⁵², A. Bursche⁴⁰, G. Busetto^{22,r}, J. Buytaert³⁸, S. Cadeddu¹⁵, R. Calabrese^{16,f}, M. Calvi^{20,k}, M. Calvo Gomez^{36,p}, A. Camboni³⁶, P. Campana^{18,38}, D. Campora Perez³⁸, A. Carbone^{14,d}, G. Carboni^{24,l}, R. Cardinale^{19,38,j}, A. Cardini¹⁵, H. Carranza-Mejia⁵⁰, L. Carson⁵⁰, K. Carvalho Akiba², G. Casse⁵², L. Cassina²⁰, L. Castillo Garcia³⁸, M. Cattaneo³⁸, Ch. Cauet⁹, R. Cenci⁵⁸, M. Charles⁸, Ph. Charpentier³⁸, S. Chen⁵⁴, S.-F. Cheung⁵⁵, N. Chiapolini⁴⁰, M. Chrzaszcz^{40,26}, K. Ciba³⁸, X. Cid Vidal³⁸, G. Ciezarek⁵³, P.E.L. Clarke⁵⁰, M. Clemencic³⁸, H.V. Cliff⁴⁷, J. Closier³⁸, V. Coco³⁸, J. Cogan⁶, E. Cogneras⁵, P. Collins³⁸, A. Comerma-Montells¹¹, A. Contu¹⁵, A. Cook⁴⁶, M. Coombes⁴⁶, S. Coquereau⁸, G. Corti³⁸, M. Corvo^{16,f}, I. Counts⁵⁶, B. Couturier³⁸, G.A. Cowan⁵⁰, D.C. Craik⁴⁸, M. Cruz Torres⁶⁰, S. Cunliffe⁵³, R. Currie⁵⁰, C. D'Ambrosio³⁸, J. Dalseno⁴⁶, P. David⁸, P.N.Y. David⁴¹, A. Davis⁵⁷, K. De Bruyn⁴¹, S. De Capua⁵⁴, M. De Cian¹¹, J.M. De Miranda¹, L. De Paula², W. De Silva⁵⁷, P. De Simone¹⁸, D. Decamp⁴, M. Deckenhoff⁹, L. Del Buono⁸, N. Déleage⁴, D. Derkach⁵⁵, O. Deschamps⁵, F. Dettori³⁸, A. Di Canto³⁸, H. Dijkstra³⁸, S. Donleavy⁵², F. Dordei¹¹, M. Dorigo³⁹, A. Dosil Suárez³⁷, D. Dossett⁴⁸, A. Dovbnya⁴³, K. Dreimanis⁵², G. Dujany⁵⁴, F. Dupertuis³⁹, P. Durante³⁸, R. Dzhelyadin³⁵, A. Dziurda²⁶, A. Dzyuba³⁰, S. Easo^{49,38}, U. Egede⁵³, V. Egorychev³¹, S. Eidelman³⁴, S. Eisenhardt⁵⁰, U. Eitschberger⁹, R. Ekelhof⁹, L. Eklund^{51,38}, I. El Rifai⁵, Ch. Elsasser⁴⁰, S. Ely⁵⁹, S. Esen¹¹, T. Evans⁵⁵, A. Falabella^{16,f}, C. Färber¹¹, C. Farinelli⁴¹, N. Farley⁴⁵, S. Farry⁵², RF Fay⁵², D. Ferguson⁵⁰, V. Fernandez Albor³⁷, F. Ferreira Rodrigues¹, M. Ferro-Luzzi³⁸, S. Filippov³³, M. Fiore^{16,f}, M. Fiorini^{16,f}, M. Firlej²⁷, C. Fitzpatrick³⁸, T. Fiutowski²⁷, M. Fontana¹⁰, F. Fontanelli^{19,j}, R. Forty³⁸, O. Francisco², M. Frank³⁸, C. Frei³⁸, M. Frosini^{17,38,g}, J. Fu^{21,38}, E. Furfaro^{24,l}, A. Gallas Torreira³⁷, D. Galli^{14,d}, S. Gallorini²², S. Gambetta^{19,j}, M. Gandelman², P. Gandini⁵⁹, Y. Gao³, J. Garofoli⁵⁹, J. Garra Tico⁴⁷, L. Garrido³⁶, C. Gaspar³⁸, R. Gauld⁵⁵, L. Gavardi⁹, G. Gavrilo³⁰, E. Gersabeck¹¹, M. Gersabeck⁵⁴, T. Gershon⁴⁸, Ph. Ghez⁴, A. Gianelle²², S. Giani³⁹, V. Gibson⁴⁷, L. Giubega²⁹, V.V. Gligorov³⁸, C. Göbel⁶⁰, D. Golubkov³¹, A. Golutvin^{53,31,38}, A. Gomes^{1,a}, H. Gordon³⁸, C. Gotti²⁰, M. Grabalosa Gándara⁵, R. Graciani Diaz³⁶, L.A. Granado Cardoso³⁸, E. Graugés³⁶, G. Graziani¹⁷, A. Grecu²⁹, E. Greening⁵⁵, S. Gregson⁴⁷, P. Griffith⁴⁵, L. Grillo¹¹, O. Grünberg⁶², B. Gui⁵⁹, E. Gushchin³³, Yu. Guz^{35,38}, T. Gys³⁸, C. Hadjivasiliou⁵⁹, G. Haefeli³⁹, C. Haen³⁸, S.C. Haines⁴⁷, S. Hall⁵³, B. Hamilton⁵⁸, T. Hampson⁴⁶, X. Han¹¹, S. Hansmann-Menzemer¹¹, N. Harnew⁵⁵, S.T. Harnew⁴⁶, J. Harrison⁵⁴, T. Hartmann⁶², J. He³⁸, T. Head³⁸, V. Heijne⁴¹, K. Hennessy⁵², P. Henrard⁵, L. Henry⁸, J.A. Hernando Morata³⁷, E. van Herwijnen³⁸, M. Heß⁶², A. Hicheur¹, D. Hill⁵⁵, M. Hoballah⁵, C. Hombach⁵⁴, W. Hulsbergen⁴¹, P. Hunt⁵⁵, N. Hussain⁵⁵,

D. Hutchcroft⁵², D. Hynds⁵¹, M. Idzik²⁷, P. Ilten⁵⁶, R. Jacobsson³⁸, A. Jaeger¹¹, J. Jalocha⁵⁵,
 E. Jans⁴¹, P. Jatton³⁹, A. Jawahery⁵⁸, F. Jing³, M. John⁵⁵, D. Johnson⁵⁵, C.R. Jones⁴⁷,
 C. Joram³⁸, B. Jost³⁸, N. Jurik⁵⁹, M. Kaballo⁹, S. Kandybei⁴³, W. Kanso⁶, M. Karacson³⁸,
 T.M. Karbach³⁸, S. Karodia⁵¹, M. Kelsey⁵⁹, I.R. Kenyon⁴⁵, T. Ketel⁴², B. Khanji²⁰,
 C. Khurewathanakul³⁹, S. Klaver⁵⁴, O. Kochebina⁷, M. Kolpin¹¹, I. Komarov³⁹, R.F. Koopman⁴²,
 P. Koppenburg^{41,38}, M. Korolev³², A. Kozlinskiy⁴¹, L. Kravchuk³³, K. Kreplin¹¹, M. Kreps⁴⁸,
 G. Krocker¹¹, P. Krokovny³⁴, F. Kruse⁹, W. Kucewicz^{26,o}, M. Kucharczyk^{20,26,38,k},
 V. Kudryavtsev³⁴, K. Kurek²⁸, T. Kvaratskheliya³¹, V.N. La Thi³⁹, D. Lacarrere³⁸, G. Lafferty⁵⁴,
 A. Lai¹⁵, D. Lambert⁵⁰, R.W. Lambert⁴², E. Lanciotti³⁸, G. Lanfranchi¹⁸, C. Langenbruch³⁸,
 B. Langhans³⁸, T. Latham⁴⁸, C. Lazzeroni⁴⁵, R. Le Gac⁶, J. van Leerdam⁴¹, J.-P. Lees⁴,
 R. Lefèvre⁵, A. Leflat³², J. Lefrançois⁷, S. Leo²³, O. Leroy⁶, T. Lesiak²⁶, B. Leverington¹¹, Y. Li³,
 M. Liles⁵², R. Lindner³⁸, C. Linn³⁸, F. Lionetto⁴⁰, B. Liu¹⁵, G. Liu³⁸, S. Lohn³⁸, I. Longstaff⁵¹,
 J.H. Lopes², N. Lopez-March³⁹, P. Lowdon⁴⁰, H. Lu³, D. Lucchesi^{22,r}, H. Luo⁵⁰, A. Lupato²²,
 E. Luppi^{16,f}, O. Lupton⁵⁵, F. Machefert⁷, I.V. Machikhiliyan³¹, F. Maciuc²⁹, O. Maev³⁰,
 S. Malde⁵⁵, G. Manca^{15,e}, G. Mancinelli⁶, J. Maratas⁵, J.F. Marchand⁴, U. Marconi¹⁴,
 C. Marin Benito³⁶, P. Marino^{23,t}, R. Märki³⁹, J. Marks¹¹, G. Martellotti²⁵, A. Martens⁸,
 A. Martín Sánchez⁷, M. Martinelli⁴¹, D. Martinez Santos⁴², F. Martinez Vidal⁶⁴,
 D. Martins Tostes², A. Massafferri¹, R. Matev³⁸, Z. Mathe³⁸, C. Matteuzzi²⁰, A. Mazurov^{16,f},
 M. McCann⁵³, J. McCarthy⁴⁵, A. McNab⁵⁴, R. McNulty¹², B. McSkelly⁵², B. Meadows⁵⁷,
 F. Meier⁹, M. Meissner¹¹, M. Merk⁴¹, D.A. Milanes⁸, M.-N. Minard⁴, N. Moggi¹⁴,
 J. Molina Rodriguez⁶⁰, S. Monteil⁵, M. Morandin²², P. Morawski²⁷, A. Mordà⁶, M.J. Morello^{23,t},
 J. Moron²⁷, A.-B. Morris⁵⁰, R. Mountain⁵⁹, F. Muheim⁵⁰, K. Müller⁴⁰, R. Muresan²⁹,
 M. Mussini¹⁴, B. Muster³⁹, P. Naik⁴⁶, T. Nakada³⁹, R. Nandakumar⁴⁹, I. Nasteva²,
 M. Needham⁵⁰, N. Neri²¹, S. Neubert³⁸, N. Neufeld³⁸, M. Neuner¹¹, A.D. Nguyen³⁹,
 T.D. Nguyen³⁹, C. Nguyen-Mau^{39,q}, M. Nicol⁷, V. Niess⁵, R. Niet⁹, N. Nikitin³², T. Nikodem¹¹,
 A. Novoselov³⁵, D.P. O'Hanlon⁴⁸, A. Oblakowska-Mucha²⁷, V. Obraztsov³⁵, S. Oggero⁴¹,
 S. Ogilvy⁵¹, O. Okhrimenko⁴⁴, R. Oldeman^{15,e}, G. Onderwater⁶⁵, M. Orlandea²⁹,
 J.M. Otalora Goicochea², P. Owen⁵³, A. Oyanguren⁶⁴, B.K. Pal⁵⁹, A. Palano^{13,c}, F. Palombo^{21,u},
 M. Palutan¹⁸, J. Panman³⁸, A. Papanestis^{49,38}, M. Pappagallo⁵¹, C. Parkes⁵⁴, C.J. Parkinson^{9,45},
 G. Passaleva¹⁷, G.D. Patel⁵², M. Patel⁵³, C. Patrignani^{19,j}, A. Pazos Alvarez³⁷, A. Pearce⁵⁴,
 A. Pellegrino⁴¹, M. Pepe Altarelli³⁸, S. Perazzini^{14,d}, E. Perez Trigo³⁷, P. Perret⁵,
 M. Perrin-Terrin⁶, L. Pescatore⁴⁵, E. Pesen⁶⁶, K. Petridis⁵³, A. Petrolini^{19,j},
 E. Picatoste Olloqui³⁶, B. Pietrzyk⁴, T. Pilar⁴⁸, D. Pinci²⁵, A. Pistone¹⁹, S. Playfer⁵⁰,
 M. Plo Casasus³⁷, F. Polci⁸, A. Poluektov^{48,34}, E. Polcarpo², A. Popov³⁵, D. Popov¹⁰,
 B. Popovici²⁹, C. Potterat², J. Prisciandaro³⁹, A. Pritchard⁵², C. Prouve⁴⁶, V. Pugatch⁴⁴,
 A. Puig Navarro³⁹, G. Punzi^{23,s}, W. Qian⁴, B. Rachwal²⁶, J.H. Rademacker⁴⁶,
 B. Rakotomiaramananana³⁹, M. Rama¹⁸, M.S. Rangel², I. Raniuk⁴³, N. Rauschmayr³⁸, G. Raven⁴²,
 S. Reichert⁵⁴, M.M. Reid⁴⁸, A.C. dos Reis¹, S. Ricciardi⁴⁹, A. Richards⁵³, M. Rihl³⁸,
 K. Rinnert⁵², V. Rives Molina³⁶, D.A. Roa Romero⁵, P. Robbe⁷, A.B. Rodrigues¹,
 E. Rodrigues⁵⁴, P. Rodriguez Perez⁵⁴, S. Roiser³⁸, V. Romanovsky³⁵, A. Romero Vidal³⁷,
 M. Rotondo²², J. Rouvinet³⁹, T. Ruf³⁸, F. Ruffini²³, H. Ruiz³⁶, P. Ruiz Valls⁶⁴, G. Sabatino^{25,l},
 J.J. Saborido Silva³⁷, N. Sagidova³⁰, P. Sail⁵¹, B. Saitta^{15,e}, V. Salustino Guimaraes²,
 C. Sanchez Mayordomo⁶⁴, B. Sanmartin Sedes³⁷, R. Santacesaria²⁵, C. Santamarina Rios³⁷,
 E. Santovetti^{24,l}, M. Sapunov⁶, A. Sarti^{18,m}, C. Satriano^{25,n}, A. Satta²⁴, M. Savrie^{16,f},
 D. Savrina^{31,32}, M. Schiller⁴², H. Schindler³⁸, M. Schlupp⁹, M. Schmelling¹⁰, B. Schmidt³⁸,
 O. Schneider³⁹, A. Schopper³⁸, M.-H. Schune⁷, R. Schwemmer³⁸, B. Sciascia¹⁸, A. Sciubba²⁵,
 M. Seco³⁷, A. Semennikov³¹, I. Sepp⁵³, N. Serra⁴⁰, J. Serrano⁶, L. Sestini²², P. Seyfert¹¹,
 M. Shapkin³⁵, I. Shapoval^{16,43,f}, Y. Shcheglov³⁰, T. Shears⁵², L. Shekhtman³⁴, V. Shevchenko⁶³,

A. Shires⁹, R. Silva Coutinho⁴⁸, G. Simi²², M. Sirendi⁴⁷, N. Skidmore⁴⁶, T. Skwarnicki⁵⁹, N.A. Smith⁵², E. Smith^{55,49}, E. Smith⁵³, J. Smith⁴⁷, M. Smith⁵⁴, H. Snoek⁴¹, M.D. Sokoloff⁵⁷, F.J.P. Soler⁵¹, F. Soomro³⁹, D. Souza⁴⁶, B. Souza De Paula², B. Spaan⁹, A. Sparkes⁵⁰, P. Spradlin⁵¹, F. Stagni³⁸, M. Stahl¹¹, S. Stahl¹¹, O. Steinkamp⁴⁰, O. Stenyakin³⁵, S. Stevenson⁵⁵, S. Stoica²⁹, S. Stone⁵⁹, B. Storaci⁴⁰, S. Stracka^{23,38}, M. Straticiuc²⁹, U. Straumann⁴⁰, R. Stroili²², V.K. Subbiah³⁸, L. Sun⁵⁷, W. Sutcliffe⁵³, K. Swientek²⁷, S. Swientek⁹, V. Syropoulos⁴², M. Szczekowski²⁸, P. Szczypka^{39,38}, D. Szilard², T. Szumlak²⁷, S. T'Jampens⁴, M. Teklishyn⁷, G. Tellarini^{16,f}, F. Teubert³⁸, C. Thomas⁵⁵, E. Thomas³⁸, J. van Tilburg⁴¹, V. Tisserand⁴, M. Tobin³⁹, S. Tolk⁴², L. Tomassetti^{16,f}, D. Tonelli³⁸, S. Topp-Joergensen⁵⁵, N. Tori⁵⁵, E. Tournefier⁴, S. Tourneur³⁹, M.T. Tran³⁹, M. Tresch⁴⁰, A. Tsaregorodtsev⁶, P. Tsopelas⁴¹, N. Tuning⁴¹, M. Ubeda Garcia³⁸, A. Ukleja²⁸, A. Ustyuzhanin⁶³, U. Uwer¹¹, V. Vagnoni¹⁴, G. Valenti¹⁴, A. Vallier⁷, R. Vazquez Gomez¹⁸, P. Vazquez Regueiro³⁷, C. Vázquez Sierra³⁷, S. Vecchi¹⁶, J.J. Velthuis⁴⁶, M. Veltri^{17,h}, G. Veneziano³⁹, M. Vesterinen¹¹, B. Viaud⁷, D. Vieira², M. Vieites Diaz³⁷, X. Vilasis-Cardona^{36,p}, A. Vollhardt⁴⁰, D. Volyansky¹⁰, D. Voong⁴⁶, A. Vorobyev³⁰, V. Vorobyev³⁴, C. Voß⁶², H. Voss¹⁰, J.A. de Vries⁴¹, R. Waldi⁶², C. Wallace⁴⁸, R. Wallace¹², J. Walsh²³, S. Wandernoth¹¹, J. Wang⁵⁹, D.R. Ward⁴⁷, N.K. Watson⁴⁵, D. Websdale⁵³, M. Whitehead⁴⁸, J. Wicht³⁸, D. Wiedner¹¹, G. Wilkinson⁵⁵, M.P. Williams⁴⁵, M. Williams⁵⁶, F.F. Wilson⁴⁹, J. Wimberley⁵⁸, J. Wishahi⁹, W. Wislicki²⁸, M. Witek²⁶, G. Wormser⁷, S.A. Wotton⁴⁷, S. Wright⁴⁷, S. Wu³, K. Wyllie³⁸, Y. Xie⁶¹, Z. Xing⁵⁹, Z. Xu³⁹, Z. Yang³, X. Yuan³, O. Yushchenko³⁵, M. Zangoli¹⁴, M. Zavertyaev^{10,b}, L. Zhang⁵⁹, W.C. Zhang¹², Y. Zhang³, A. Zhelezov¹¹, A. Zhokhov³¹, L. Zhong³ and A. Zvyagin³⁸.

¹ *Centro Brasileiro de Pesquisas Físicas (CBPF), Rio de Janeiro, Brazil*

² *Universidade Federal do Rio de Janeiro (UFRJ), Rio de Janeiro, Brazil*

³ *Center for High Energy Physics, Tsinghua University, Beijing, China*

⁴ *LAPP, Université de Savoie, CNRS/IN2P3, Annecy-Le-Vieux, France*

⁵ *Clermont Université, Université Blaise Pascal, CNRS/IN2P3, LPC, Clermont-Ferrand, France*

⁶ *CPPM, Aix-Marseille Université, CNRS/IN2P3, Marseille, France*

⁷ *LAL, Université Paris-Sud, CNRS/IN2P3, Orsay, France*

⁸ *LPNHE, Université Pierre et Marie Curie, Université Paris Diderot, CNRS/IN2P3, Paris, France*

⁹ *Fakultät Physik, Technische Universität Dortmund, Dortmund, Germany*

¹⁰ *Max-Planck-Institut für Kernphysik (MPIK), Heidelberg, Germany*

¹¹ *Physikalisches Institut, Ruprecht-Karls-Universität Heidelberg, Heidelberg, Germany*

¹² *School of Physics, University College Dublin, Dublin, Ireland*

¹³ *Sezione INFN di Bari, Bari, Italy*

¹⁴ *Sezione INFN di Bologna, Bologna, Italy*

¹⁵ *Sezione INFN di Cagliari, Cagliari, Italy*

¹⁶ *Sezione INFN di Ferrara, Ferrara, Italy*

¹⁷ *Sezione INFN di Firenze, Firenze, Italy*

¹⁸ *Laboratori Nazionali dell'INFN di Frascati, Frascati, Italy*

¹⁹ *Sezione INFN di Genova, Genova, Italy*

²⁰ *Sezione INFN di Milano Bicocca, Milano, Italy*

²¹ *Sezione INFN di Milano, Milano, Italy*

²² *Sezione INFN di Padova, Padova, Italy*

²³ *Sezione INFN di Pisa, Pisa, Italy*

²⁴ *Sezione INFN di Roma Tor Vergata, Roma, Italy*

²⁵ *Sezione INFN di Roma La Sapienza, Roma, Italy*

²⁶ *Henryk Niewodniczanski Institute of Nuclear Physics Polish Academy of Sciences, Kraków, Poland*

²⁷ *AGH - University of Science and Technology, Faculty of Physics and Applied Computer Science, Kraków, Poland*

²⁸ *National Center for Nuclear Research (NCBJ), Warsaw, Poland*

- ²⁹ Horia Hulubei National Institute of Physics and Nuclear Engineering, Bucharest-Magurele, Romania
- ³⁰ Petersburg Nuclear Physics Institute (PNPI), Gatchina, Russia
- ³¹ Institute of Theoretical and Experimental Physics (ITEP), Moscow, Russia
- ³² Institute of Nuclear Physics, Moscow State University (SINP MSU), Moscow, Russia
- ³³ Institute for Nuclear Research of the Russian Academy of Sciences (INR RAN), Moscow, Russia
- ³⁴ Budker Institute of Nuclear Physics (SB RAS) and Novosibirsk State University, Novosibirsk, Russia
- ³⁵ Institute for High Energy Physics (IHEP), Protvino, Russia
- ³⁶ Universitat de Barcelona, Barcelona, Spain
- ³⁷ Universidad de Santiago de Compostela, Santiago de Compostela, Spain
- ³⁸ European Organization for Nuclear Research (CERN), Geneva, Switzerland
- ³⁹ Ecole Polytechnique Fédérale de Lausanne (EPFL), Lausanne, Switzerland
- ⁴⁰ Physik-Institut, Universität Zürich, Zürich, Switzerland
- ⁴¹ Nikhef National Institute for Subatomic Physics, Amsterdam, The Netherlands
- ⁴² Nikhef National Institute for Subatomic Physics and VU University Amsterdam, Amsterdam, The Netherlands
- ⁴³ NSC Kharkiv Institute of Physics and Technology (NSC KIPT), Kharkiv, Ukraine
- ⁴⁴ Institute for Nuclear Research of the National Academy of Sciences (KINR), Kyiv, Ukraine
- ⁴⁵ University of Birmingham, Birmingham, United Kingdom
- ⁴⁶ H.H. Wills Physics Laboratory, University of Bristol, Bristol, United Kingdom
- ⁴⁷ Cavendish Laboratory, University of Cambridge, Cambridge, United Kingdom
- ⁴⁸ Department of Physics, University of Warwick, Coventry, United Kingdom
- ⁴⁹ STFC Rutherford Appleton Laboratory, Didcot, United Kingdom
- ⁵⁰ School of Physics and Astronomy, University of Edinburgh, Edinburgh, United Kingdom
- ⁵¹ School of Physics and Astronomy, University of Glasgow, Glasgow, United Kingdom
- ⁵² Oliver Lodge Laboratory, University of Liverpool, Liverpool, United Kingdom
- ⁵³ Imperial College London, London, United Kingdom
- ⁵⁴ School of Physics and Astronomy, University of Manchester, Manchester, United Kingdom
- ⁵⁵ Department of Physics, University of Oxford, Oxford, United Kingdom
- ⁵⁶ Massachusetts Institute of Technology, Cambridge, MA, United States
- ⁵⁷ University of Cincinnati, Cincinnati, OH, United States
- ⁵⁸ University of Maryland, College Park, MD, United States
- ⁵⁹ Syracuse University, Syracuse, NY, United States
- ⁶⁰ Pontifícia Universidade Católica do Rio de Janeiro (PUC-Rio), Rio de Janeiro, Brazil, associated to ²
- ⁶¹ Institute of Particle Physics, Central China Normal University, Wuhan, Hubei, China, associated to ³
- ⁶² Institut für Physik, Universität Rostock, Rostock, Germany, associated to ¹¹
- ⁶³ National Research Centre Kurchatov Institute, Moscow, Russia, associated to ³¹
- ⁶⁴ Instituto de Fisica Corpuscular (IFIC), Universitat de Valencia-CSIC, Valencia, Spain, associated to ³⁶
- ⁶⁵ KVI - University of Groningen, Groningen, The Netherlands, associated to ⁴¹
- ⁶⁶ Celal Bayar University, Manisa, Turkey, associated to ³⁸
- ^a Universidade Federal do Triângulo Mineiro (UFTM), Uberaba-MG, Brazil
- ^b P.N. Lebedev Physical Institute, Russian Academy of Science (LPI RAS), Moscow, Russia
- ^c Università di Bari, Bari, Italy
- ^d Università di Bologna, Bologna, Italy
- ^e Università di Cagliari, Cagliari, Italy
- ^f Università di Ferrara, Ferrara, Italy
- ^g Università di Firenze, Firenze, Italy
- ^h Università di Urbino, Urbino, Italy

- ⁱ *Università di Modena e Reggio Emilia, Modena, Italy*
- ^j *Università di Genova, Genova, Italy*
- ^k *Università di Milano Bicocca, Milano, Italy*
- ^l *Università di Roma Tor Vergata, Roma, Italy*
- ^m *Università di Roma La Sapienza, Roma, Italy*
- ⁿ *Università della Basilicata, Potenza, Italy*
- ^o *AGH - University of Science and Technology, Faculty of Computer Science, Electronics and Telecommunications, Kraków, Poland*
- ^p *LIFAELS, La Salle, Universitat Ramon Llull, Barcelona, Spain*
- ^q *Hanoi University of Science, Hanoi, Viet Nam*
- ^r *Università di Padova, Padova, Italy*
- ^s *Università di Pisa, Pisa, Italy*
- ^t *Scuola Normale Superiore, Pisa, Italy*
- ^u *Università degli Studi di Milano, Milano, Italy*